

Final Technical Report for Year 5 Early Career Research Project “Viscosity and equation of state of hot and dense QCD matter”

Period: 04/15/2014 - 04/14/2015 (5th year, with no-cost extension until 08/14/2015)

DOE Award: DE-SC0004035

Principal Investigator (PI): Denes Molnar, Purdue University

1 Main research activities and accomplishments

The Section below summarizes research activities and achievements during the fifth (last) year of the PI's Early Career Research Project (ECRP). Unlike the first four years of the project, the last year was not funded under the American Recovery and Reinvestment Act (ARRA). The ECRP advanced two main areas: i) radiative $3 \leftrightarrow 2$ radiative transport, via development of a new computer code MPC/Grid that solves the Boltzmann transport equation in full 6+1D (3X+3V+time); and ii) application of relativistic hydrodynamics, via development of a self-consistent framework to convert viscous fluids to particles. In Year 5 we finalized thermalization studies with radiative $gg \leftrightarrow ggg$ transport (Sec. 1.1.1) and used nonlinear covariant transport to assess the accuracy of fluid-to-particle conversion models (Sec. 1.1.2), calculated observables with self-consistent fluid-to-particle conversion from realistic viscous hydrodynamic evolution (Secs. 1.2.1 and 1.2.2), extended the covariant energy loss formulation to heavy quarks (Sec. 1.4.1) and studied energy loss in small systems (Sec. 1.4.2), and also investigated how much of the elliptic flow could have non-hydrodynamic origin (Sec 1.3). Years 1-4 of the ECRP were ARRA-funded and, therefore, they have their own report document 'Final Technical Report for Years 1-4 of the Early Career Research Project "Viscosity and equation of state of hot and dense QCD matter"' (same award number DE-SC0004035).

The PI's group was also part of the DOE JET Topical Collaboration, a multi-institution project that overlapped in time significantly with the ECRP. Purdue achievements as part of the JET Topical Collaboration are in a separate report "Final Technical Report summarizing Purdue research activities as part of the DOE JET Topical Collaboration" (award DE-SC0004077).

1.1 Radiative $3 \leftrightarrow 2$ transport

A striking feature of ultra-relativistic heavy ion collisions is that experimental data indicate the creation of a hot and dense system created that is nearly thermal and has very small viscosity. This lead to emergence of the strongly coupled quark-gluon plasma (sQGP) paradigm[1]. Indeed, quark-gluon kinetic theory has had for a long time big difficulty with fast thermalization with on-shell $2 \rightarrow 2$ rates (see, e.g., [2]) based on perturbative quantum-chromodynamics (pQCD) cross sections. There has been a striking outstanding claim[3], however, based on the Boltzmann Approach to Multi-Particle Scattering (BAMPS) code, that the inclusion of radiative $ggg \leftrightarrow gg$ rates can shorten thermalization time-scales in $A + A$ at Relativistic Heavy Ion Collider (RHIC) and Large Hadron Collider (LHC) by nearly an order of magnitude. The results were controversial because it was argued (e.g., [4, 5]) that the BAMPS calculation may have overestimated the rates by a factor of $3! = 6$.

A key achievement of the ECRP was the development of a new computer package MPC/Grid that solves on-shell Boltzmann transport with elastic $2 \rightarrow 2$ and radiative $2 \leftrightarrow 3$ interactions (MPC stands for Molnar's Parton Cascade). With MPC/Grid we reinvestigated the BAMPS results, and found about $5\times$ smaller rates and much longer rapid thermalization timescales than those published with BAMPS, even with matrix elements in the same Bertsch-Gunion[6] approximation. These comparisons, however, revealed that $gg \leftrightarrow ggg$ rates are highly sensitive to the value of the Debye mass, and how Debye screening and the Landau-Pomerantchuk-Migdal (LPM) destructive interference[7, 8, 9] are implemented.

In Year 5 we finalized the studies of thermalization at RHIC from MPC/Grid, improved the self-consistent determination of the Debye mass, and ported most features of the single CPU version of MPC/Grid into the parallelized version. We then used MPC/Grid to compute shear viscous phasespace corrections from nonlinear transport, and investigated how accurately different fluid-to-particle conversion models can reconstruct the real particle distributions in the transport solely from the hydrodynamic fields. This work was done by graduate students Dustin Hemphill and Mridula Damodaran.

1.1.1 Covariant Boltzmann solver MPC/Grid

One shortcoming of our preliminary thermalization results for conditions in Au+Au at RHIC was that outgoing particle momenta in $2 \leftrightarrow 3$ scatterings were generated isotropically instead of according to the pQCD matrix elements. This speeds up calculations because isotropic momenta can be generated with 100% efficiency. Thermal rates were unaffected because the energy dependence of the total $2 \rightarrow 3$ cross section $\sigma_{gg \rightarrow ggg}(s)$ was properly tabulated and already included. But far away from equilibrium the shortcut may matter because it affects how phase space gets populated by randomization of momenta during the evolution. Heuristically, one expects that isotropic generation leads to more rapid thermalization and larger elliptic flow because it randomizes momenta better, but this did not deflect criticism that perhaps those expectations are wrong.

To remedy this we had to port most of the features from the single-CPU version of MPC/Grid into the parallel one, especially the Bertsch-Gunion momentum generator so that we could run these studies on multiple cores (the two codes have diverged significantly over the years because they have been developed by different students, and communication needs in the multi-CPU case also change the natural program flow). Once the port was finished, both static box thermalization studies and calculations of elliptic flow in Au+Au at RHIC were redone. Surprisingly, results changed very little compared to those with the much faster, isotropic outgoing momentum generation. The most likely reason is that at temperatures at RHIC, and even the LHC, the Debye mass μ_D is not that small, therefore, typical scatterings are not very forward peaked ($\mu_D^2/s \sim g^2 T^2 / 18T^2 \sim 0.2$).

Just like in earlier findings, thermalization was much more rapid for self-consistent dynamical

$$\mu_D^2[f] = 3\pi\alpha_s \int d^3p \frac{1}{p} f(\vec{p}) \quad (1)$$

from linear response theory[10]. Therefore, we looked very carefully into the determination of μ_D . Equation (1) means in practice a sum over test particles in a volume V : $\mu_D = 3\pi\alpha_s/\ell V \times \sum_i 1/p_i$, where ℓ is the oversampling factor. In principle this should be evaluated locally in small volumes, but that requires prohibitively many test particles in order to suppress finite number fluctuations. Therefore, as does BAMPS, we compute an average μ_D for slices of the system in the longitudinal coordinate z , which then needs an estimated V for each slice. The larger the volume, the smaller the average Debye mass will be. BAMPS used particles in a transverse disc of an arbitrary radius $R = 6$ fm. MPC/Grid takes instead the combined volume of all nonempty cells in the transverse

slice, which has the benefit that it adapts automatically as the effective transverse size of the system changes. We realized, however, that oversampling gives larger V because sampling more test particles from the same spatial distribution leads to more occupied cells on average. Two more robust methods were, therefore, implemented: one calculates the second moments $R_x^2 = \langle x^2 \rangle$ and $R_y^2 = \langle y^2 \rangle$ of transverse coordinates, and takes $V \propto \pi(2R_x)(2R_y)$, the other requires at least ℓ particles in a cell to consider it occupied. In practice both methods led to smaller volumes, i.e., larger μ_D , and thus weaker thermalization and collective effects.

These results were presented at Quark Matter 2015 (Sep 2015), and will be an integral part of Dustin Hemphill's Ph.D. thesis.

1.1.2 Viscous corrections from nonlinear transport

With the parallel version of MPC/Grid we performed transport calculations with exceptionally high statistics, nearly 10^9 test particles, in order to test viscous correction (δf) models used in comparisons of relativistic viscous hydrodynamics to data against realistic corrections from nonlinear $2 \rightarrow 2$ transport. Such δf models try to reconstruct the full phase space distribution of each particle species from knowledge of the hydrodynamic fields alone, which is a challenge even for a system of only a single species[11] (a self-consistent approach to this problem is in Sec. 1.2). We chose a longitudinally boost invariant one-component system undergoing 0+1D Bjorken expansion for this study because then the phase space distribution $f(p_T, \xi, \tau)$ only depends on transverse momentum p_T and the difference between coordinate and momentum rapidities $\xi = \eta - y$ at any proper time $\tau = \sqrt{t^2 - z^2}$ (see [12] for an extensive discussion of this scenario). There are only three independent hydrodynamic fields in this case: pressure $p(\tau)$, number density $n(\tau) = n_0 \tau_0 / \tau$, and longitudinal shear stress $\pi_L(\tau)$. Transport solutions only depend on the dimensionless inverse Knudsen number $K(\tau) = \sigma n \tau = \sigma n_0 \tau_0$, which also controls the shear viscosity $\eta/s \sim \tau^{2/3}/K(\tau)$.

We compared against four δf models: power-law generalizations of the Grad ansatz

$$\delta f = \text{const} \times (p \cdot u)^{\alpha-2} \pi^{\mu\nu} p_\mu p_\nu f^{\text{eq}} \quad (2)$$

with i) $\alpha = 1$ (linear $\propto p^1$), ii) $\alpha = 3/2$ (i.e., $\propto p^{1.5}$), and iii) $\alpha = 2$ (quadratic p^2); and iv) the Strickland-Romatschke (SR) form[13] $f = f^{\text{eq}} + \delta f \propto e^{-p_T \sqrt{\text{ch}^2 \xi + \text{ash}^2 \xi} / \Lambda}$. The quadratic case corresponds to the commonly used Grad ansatz, $p^{1.5}$ corresponds to our self-consistent corrections in Sec. 1.2, linear dependence arises when transport equation is treated in the relaxation time approximation (see, e.g., [14]), while the SR form is exact for a gas expanding without any interactions (free streaming). All these forms contain three adjustable parameters, which are completely fixed by the hydrodynamic quantities p , n , and π_L .

To simulate boost invariant evolution, numerical solutions were calculated with MPC/Grid from locally thermal initial conditions with uniform coordinate rapidity density $dN/d\eta = \text{const}$ in a wide window $|\eta| < 5$. For simplicity, massless particles were considered. In the analysis only those 20% of test particles were used that had $|\eta| < 1$ at the given τ (about 190 million useful counts at each τ). We investigated both $\sigma = \text{const}$ and growing $\sigma \propto \tau^{2/3}$ scenarios (the latter maintain $\eta/s \approx \text{const}$). To test the accuracy of δf models, from the full transport evolution $f_{tr}(p_T, \xi)$ at various values of τ we calculated p , n , and π_L from the number current $N^\mu = \int d^3 p p^\mu f/E$ and the energy-momentum tensor $T^{\mu\nu} = \int d^3 p p^\mu p^\nu f/E$, and used those to construct phase space density predictions from each of the four δf models. The reconstructed distributions f_{rec} were then compared at each τ in rectangular bins over the $p_T - \xi$ plane to binned distributions of the numerical transport solution. We analyzed the relative error ($f_{rec}/f_{tr} - 1$) as a function of p_T and ξ , which is the most differential measure of accuracy, relative errors in integrated 1D projections $dN/d\xi$ and dN/dp_T , and finally

the single mean RMS error

$$\epsilon(\tau) = \sqrt{\frac{1}{N_{pT} N_\xi} \sum_{i,j} \left(\frac{f_{rec}(p_{T,i}, \xi_j, \tau)}{f_{tr}(p_{T,i}, \xi_j, \tau)} - 1 \right)^2} \quad (3)$$

for each time slice.

None of the δf models were found generally accurate even for very small $\eta/s \approx 0.03$ ($K_0 = 6.67$). At late times and for small viscosity, the self-consistent correction of Sec. 1.2 was most accurate (it was derived precisely for such a Navier-Stokes regime). At very early times and for large viscosities, in general, the SR form was best because in that case the evolution is closest to free streaming (for our initial conditions the initial evolution is always like free streaming because in local thermal equilibrium the Boltzmann collision term vanishes). At high momenta, errors for the power-law form (2) can get very large because the “corrections” can completely dominate the reconstructed distribution. They can even drive f_{rec} negative, which is unphysical. To remedy this, we proposed “exponentiation” analogously to $1 + x \rightarrow e^x \rightarrow e^{\text{thx}}$, where the tangent hyperbolic function is introduced to keep distributions integrable. Figure 1 (left) shows the mean RMS error for such exponentiated distributions and the SR form for $\eta/s \approx 0.2$, the highest viscosity we calculated for. At early times the SR distribution is most accurate (green dashes), while at late times the self-consistent $p^{1.5}$ power-law is best (magenta dash-dotted). The correction with linear power (blue dots) is very close to the SR form, while the most commonly used quadratic Grad ansatz (red solid lines) is the least accurate. For $\eta/s \approx 0.1$, the accuracy of the power-law forms improves by about a factor of 2, and $p^{1.5}$ becomes the most accurate (on average) at all times.

There is a residual systematic error of 5-10%, which can be regarded as a lower bound on the current theoretical uncertainty in converting viscous fluids to particles. In fact, we found that appropriately rescaled transport distributions from the same simulation at different times but with the same π_L/p exhibit $\sim 5 - 10\%$ differences, which cannot be reconstructed from hydrodynamics *even in principle* because hydrodynamic quantities are equivalent at those two times. This indicates that the system has memory. Figure 1 (right panel) shows that these effects can be captured to some extent if we extend the three-parameter δf form (green dashed) with one additional parameter (solid red). We managed to relate this extra parameter to the time derivative of π_L/p , which suggests that it is possible to include such memory effects in the fluid-to-particle conversion in standard hydrodynamic studies.

These results have been presented at the 6th Workshop of the APS GHP (Apr 2015) and at the 15th Zimányi School (Dec 2015), and are being prepared for publication.

1.2 Self-consistent conversion of viscous fluids to particles

The commonly used dynamical framework to access properties of the hot and dense matter created in ultrarelativistic heavy ion collisions is viscous hydrodynamics (see, e.g., [15, 16, 17]). Comparisons with experimental data, however, necessitate the conversion of the fluid (hydrodynamic fields) to particles, which requires additional theory ingredients not included in hydrodynamics. The commonly used “democratic” Grad method[18] of fluid-to-particle conversion is an *ad hoc* procedure that ignores completely the microscopic dynamics, in particular, that the distributions of different species deviate to different degree from local thermal equilibrium (but at least it does not violate energy and momentum conservation). The second main achievement of the ECRP was the development of a self-consistent approach[11, 19, 20] based on linearized kinetic theory to convert shear viscous fluids to particles, application of the approach to a mixture of hadrons, and study sensitivity of observables in heavy ion collisions to the conversion model.

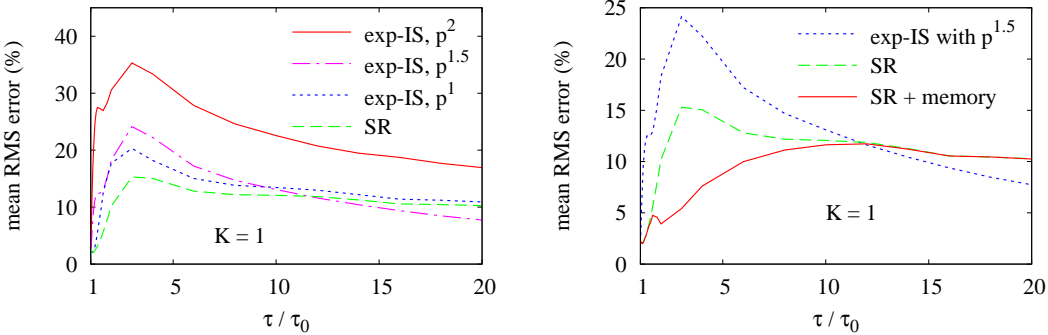


Figure 1: *Left*: mean RMS error relative to the exact distribution from nonlinear transport, for inverse Knudsen number $K = 1 \times (\tau / \tau_0)^{2/3}$. *Right*: improvement in RMS error with accounting for memory effects.

In Year 5, we extended the analysis with realistic, viscous hydrodynamic simulations for Au+Au collisions at the RHIC and Pb+Pb at the LHC, calculated higher order azimuthal flow harmonics $v_n = \langle \cos n\phi \rangle$ ($n = 4, 6$), and quantified errors in the shear viscosity to entropy density ratio η/s if it is extracted using fluid-to-particle conversion with the standard naive approach. This work was done by graduate student Zack Wolff, who graduated with a Ph.D. in Dec 2015.

1.2.1 Viscous corrections with realistic viscous hydrodynamics solutions

In Years 1-4 of the ECRP we assessed the influence of self-consistent fluid-to-particle conversion on observables in Au+Au at RHIC using hydrodynamic solutions obtained with our patched version of the AZHYDRO code[21, 22, 23, 24]. This is an ideal (non viscous) hydrodynamic code, therefore, shear stress had to be estimated[11] from flow gradients using the Navier-Stokes value $\pi^{\mu\nu} = \eta[\nabla^\mu u^\nu + \nabla^\nu u^\mu - (2/3)\Delta^{\mu\nu}(\partial \cdot u)]$. In Year 5 we performed a more realistic study with actual viscous hydrodynamic solutions, both for Au+Au at RHIC and Pb+Pb at the LHC. The viscous solutions were obtained from Harri Niemi (the same solutions were employed in [25, 26, 27, 28]). Before we could use these, two issues had to be addressed. First, the solutions were for an equation of state with a “chemically frozen” hadron gas, in which particle abundances are artificially modified below a chemical freezeout temperature $T_{chem} = 175$ MeV such that abundance ratios of various species stay the same as what they were at $T = T_{chem}$. This affects particle densities for $T < T_{chem}$, and therefore, our 49-species self-consistent viscous corrections had to be recalculated. Second, unlike the AZHYDRO equidistant space time grid output used earlier, this time only Cooper-Frye hypersurface information was provided with crude granularity, therefore, a more sophisticated, higher-order (cubic) interpolation scheme had to be devised in the integration over the hypersurface to calculate particle spectra.

We calculated harmonic flow coefficients $v_n(p_T) = \langle \cos n\phi \rangle$ for $n = 2, 4$, and 6 , with fluid-to-particle conversion at temperatures $T = 100, 120, 140$, and 160 MeV for the same 49-species hadronic mixture as in Ref. [11], using self-consistent viscous corrections with $\delta f / f^{eq} \propto p^{1.5}$ momentum dependence and additive quark model (AQM) cross sections (meson-meson, meson-baryon, and baryon-baryon cross section ratios $\sigma_{MM} : \sigma_{MB} : \sigma_{BB} = 4 : 6 : 9$). First we studied, quantitatively, the errors made in η/s extraction from $v_2(p_T)$. Figure 2 (left) illustrates our general

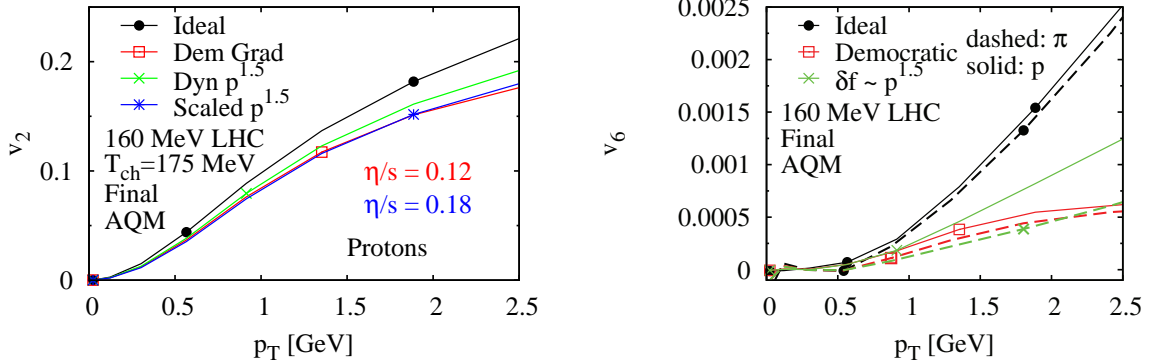


Figure 2: *Left:* systematic error in η/s extraction with the standard “democratic” Grad method from differential proton elliptic flow $v_2(p_T)$ in $\text{Pb}+\text{Pb}$ at $\sqrt{s_{NN}} = 2.76$ TeV at the LHC. *Right:* particle species dependence of the differential sixth order flow harmonic $v_6(p_T)$ in $\text{Pb}+\text{Pb}$ at $\sqrt{s_{NN}} = 2.76$ TeV at the LHC with self-consistent conversion to particles.

findings. Qualitatively, self-consistent corrections had a smaller effect on v_2 for the Niemi *et al* viscous hydro solutions than what was estimated earlier based on AZHYDRO. For conversion at $T = 160$ MeV, with $\eta/s = 0.12$, the self-consistent result for protons (green line with cross) is above the commonly used “democratic” Grad result (red line with open box). The difference may look small but it is very significant because what matters for viscosity determination is the suppression relative to the nonviscous result (black line with filled circle). In fact, the standard extraction systematically underpredicts the shear viscosity, by almost exactly 30%. To get the same level of suppression of v_2 , with self-consistent conversion one must use a 50% higher viscosity, $\eta/s = 0.18$ (blue line with star).

1.2.2 Species dependence of higher flow harmonics

Second, we analyzed the species dependence of the fourth and sixth flow harmonics v_4 and v_6 . This was especially interesting because earlier results based on AZHYDRO showed[19] big pion-proton difference in v_6 , even in the sign of v_6 . Realistic viscous hydro solutions yielded quantitatively quite different results. This was not unexpected because both v_4 and v_6 are small and are, therefore, sensitive to details of the calculation, such as the initial geometry or the conversion temperature. Nevertheless, self-consistent conversion to particles had very significant effect, especially on proton v_6 as shown in Fig. 2 (right panel) for $\text{Pb}+\text{Pb}$ at the LHC with $T_{conv} = 160$ MeV. While the sign of v_6 is now positive for both pions and protons (green lines), the magnitudes differ by almost a factor of 2. In fact, compared to ideal nonviscous conversion (black lines in Fig. 2), v_4 and v_6 were largely suppressed by viscosity even when the naive “democratic” Grad conversion was used (red lines in Fig. 2).

Results in Section 1.2 are included in Zack Wolff’s Ph.D thesis[20], and are being prepared for publication.

1.3 Investigations of whether elliptic flow really comes from hydrodynamics

We also explored the question of whether, or how much of, the observed azimuthal momentum anisotropy v_2 really comes from hydrodynamics. First, we investigated in a toy model the momentum anisotropy generated by spatial anisotropy due to quantum mechanics. Based on the uncertainty principle, one estimates for a system in its ground state $\langle p_x^2 \rangle \sim 1/\langle x^2 \rangle$, and $\langle p_y^2 \rangle \sim 1/\langle y^2 \rangle$, which implies a momentum space anisotropy $v_2 = \langle p_x^2 - p_y^2 \rangle / \langle p_x^2 + p_y^2 \rangle$ that is *equal* to the spatial eccentricity $\varepsilon = \langle y^2 - x^2 \rangle / \langle x^2 + y^2 \rangle$. This anisotropy comes purely from the wave function, it is a wave phenomenon. At nonzero temperature, of course, excited states also contribute and the uncertainty relation estimates are no longer valid. In Ref. [29] we calculated the effect in statistical physics for particles of mass M in a 2D Gaussian trap and found nonzero $v_2 \approx \varepsilon / (12MT\langle x^2 \rangle)$. The anisotropy is inherently connected to the quantization of energy levels, and thus vanishes in the high temperature limit. For typical dimensions and temperatures of the collision zone in Au+Au at RHIC, differential elliptic flow $v_2(p_T)$ was over 10% for pions above $p_T > 1$ GeV from this simple calculation. Similar effect must be present in cold fermionic gases in anisotropic traps but the magnitude of the effect is much weaker. In this sense ultracold gases are much hotter than the quark-gluon plasma. We are currently relaxing the nonrelativistic approximation, and then the results will be published.

Another striking result we demonstrated is that in the transport models such as AMPT[30, 31] or MPC[32], momentum anisotropy is largely generated not by hydrodynamic pressure gradients but, rather, by anisotropic escape from the collision zone (AMPT stands for A Multi-Particle Transport). Particles that move along the shorter x direction have less material to travel through and, therefore, they are more likely to escape than those moving in the longer y direction. The interacting (hydrodynamic) component only dominates at very high opacities $\langle N_{coll} \rangle \sim 40$. A key ingredient of the analysis was to classify particles into a noninteracting (frozen-out) component and a still interacting (hydrodynamic) one, and analyze elliptic flow for the two groups separately. This was done both as a function of the number of collisions, and also as a function of time. In both cases, the interacting component showed near zero or even negative v_2 , whereas most of the v_2 was carried by the frozen out part, even at early times. These very exciting results were published in [33], and have spurred a chain of follow-up studies as well.

1.4 Jet energy loss studies with realistic medium evolution from transport

Energetic quarks and gluons (collectively, partons) provide tomographic information about the hot and dense medium they traverse. Understanding parton energy loss in ultrarelativistic heavy-ion reactions has been the focus of considerable recent theoretical effort. A critical step in computing heavy-ion observables from any energy loss model is spatial and temporal averaging over the bulk medium formed in the collision. Purdue was the first to demonstrate[34, 35] the importance of this for the Gyulassy-Levai-Vitev (GLV) approach[36, 37, 38] to gluon and light quark energy loss. Realistic longitudinal *and* the previously ignored transverse expansion of the medium lead to a spectacular factor of two suppression in pion azimuthal momentum anisotropy v_2 (“elliptic flow”) at high p_T from GLV energy loss. We then showed that this suppression is largely compensated if one includes proper covariant treatment of energy loss in GLV or in dE/dL formulations[39].

In the final year of the ECRP we extended the covariant approach to heavy quark energy loss in the Djordjevic-Gyulassy-Levai-Vitev (DGLV) formalism[40, 41] (a moderate expansion of scope that was approved by the DOE). Heavy quarks provide a stringent cross-check for energy loss theory because, perturbatively at least, the quark mass dependence of energy loss is calculable and, therefore, all model parameters are completely fixed by light hadron observables (there are no

free parameters left to dial to match heavy quark observables). We also investigated energy loss in small systems formed in proton-nucleus (p+A) collisions. These are interesting because, shockingly, very central p+Pb events appear to behave hydrodynamically[42] at the LHC at $\sqrt{s_{NN}} = 5.02$ TeV despite the small transverse size, and energy loss provides independent, parameter-free cross-checks of the hydrodynamic interpretation. This work was performed by graduate student Deke Sun.

1.4.1 Covariant DGLV energy loss (massive quarks)

The DGLV formalism[40, 41] extends the GLV approach to heavy quarks. Even when realistic recoil of medium partons included[41], the result for the spectrum of medium induced gluon radiation at first order in opacity has a form quite similar GLV energy loss:

$$x \frac{dN_{DGLV}^{(1)}}{dx d\mathbf{k}} = \frac{C_R \alpha_s}{\pi^2} \chi \frac{x}{x_+} J \int \frac{d\mathbf{q}}{\pi} \frac{\mu^2}{\mathbf{q}^2(\mathbf{q}^2 + \mu^2)} \frac{2\mathbf{Q}}{\mathbf{Q}^2 + X} \left(\frac{\mathbf{Q}}{\mathbf{Q}^2 + X} - \frac{\mathbf{k}}{\mathbf{k}^2 + X} \right) (1 - \cos \omega z) , \quad (4)$$

where

$$\omega \equiv \frac{\mathbf{Q}^2 + X}{2Ex} , \quad \mathbf{Q} \equiv \mathbf{k} + \mathbf{q} , \quad X \equiv x_+^2 M^2 + \frac{(1 - x_+) \mu^2}{2} \approx x_+^2 M^2 , \quad J \equiv \partial x_+ / \partial x . \quad (5)$$

Here $x_+ \equiv (k^0 + k^z)/2E$ is the positive fractional light cone momentum of the radiative gluon, and J is a Jacobian between fractional light cone momentum x_+ and fractional energy x (see Refs. [40, 43] for more detail). We drop the last term in X so that the massless $M \rightarrow 0$ limit reproduces GLV energy loss apart from the replacement of the strongly screened Yukawa potential term $1/(\mathbf{q}^2 + \mu^2)^2$ with the weaker “dynamically screened” form $1/\mathbf{q}^2(\mathbf{q}^2 + \mu^2)$ (the $\mathbf{q} \rightarrow \mathbf{0}$ limit and the integral in (4) are still finite).

Integration over radiated momenta yields the average radiative DGLV energy loss for scattering at z :

$$\Delta E_{DGLV}^{(1)}(z) = \int dx d^2\mathbf{k} E x \frac{dN_{DGLV}^{(1)}}{dx d^2\mathbf{k}} = \frac{2C_R \alpha_s}{\pi} E \chi I \left(b = \frac{z}{\tau(z)}, \epsilon = \frac{E}{\mu(z)}, m \equiv \frac{M}{\mu(z)} \right) , \quad (6)$$

where we precalculate and tabulate the three dimensional function I so that $I(b, \epsilon, m)$ values can be obtained later via interpolation without major computational challenge. The deterministic average energy loss is the average of $\Delta E_{DGLV}^{(1)}(z)$ over the given jet pass:

$$\langle \Delta E^{(1)} \rangle = \frac{2C_R \alpha_s}{\pi} \int dz \rho(z) \sigma_{gg}(z) E I(z) . \quad (7)$$

The energy loss (7) is not covariant because (4) was derived for a medium at rest. Therefore, we constructed a covariant formulation using the technique we developed in Ref. [35] for GLV, i.e., demanding that (6) applies in the rest frame of the fluid element at the point of scattering z , and for other observers all quantities must then be appropriately Lorentz boosted. Just like for light partons[39], the line element $dz \rho \sigma_{gg}$ becomes $dz \rho \sigma_{gg} (1 - \vec{v} \vec{v}_F)$, i.e., covariant energy loss depends on the relative orientation of medium flow \vec{v}_F and jet velocity \vec{v} . Calculations for massive partons, however, are more involved because boosts back and forth do not combine explicitly into a compact expression. Instead, for each line element in (7), the quark momentum has to be boosted numerically to the fluid rest frame, where the DGLV energy loss (6) is evaluated, with which one computes the final quark momentum after energy loss in the fluid rest frame, and then boosts the final quark momentum back to the laboratory frame.

1.4.2 Covariant results for D and B mesons

With the covariant DGLV formulation, we calculated D and B meson observables in Au+Au at RHIC. For the medium we used, as in [39], 2+1D viscous hydrodynamic evolution with both longitudinal and transverse expansion (fKLN initial profile, shear viscosity to entropy density ratio $\eta/s = 0.08$), and α_s was set to reproduce the neutral pion suppression factor R_{AA} . Figure 3 shows our results for differential elliptic flow for D (left plot) and B mesons (right plot), calculated using DGLV energy loss for charm and bottom quarks ($M = 1.5$ and 4.5 GeV), followed by independent fragmentation using Peterson fragmentation functions[44] with $\epsilon_c = 0.06$ and $\epsilon_b = 0.005$ as in Ref. [43]. We found that jet-medium flow coupling in covariant energy loss (solid green) also increases v_2 for heavy flavor compared to noncovariant DGLV energy loss (dotted blue). For B mesons at high p_T , the effect is close to the nearly $2\times$ enhancement we got earlier for pions [39], but for charm, and bottom at low p_T , it is much smaller. In addition, we observed negligible difference due to covariance in the D meson R_{AA} but there was a noticeable 5-10% reduction in B meson R_{AA} . (The dashed red lines in Fig. 3 are for longitudinal expansion only with the original, noncovariant DGLV energy loss.)

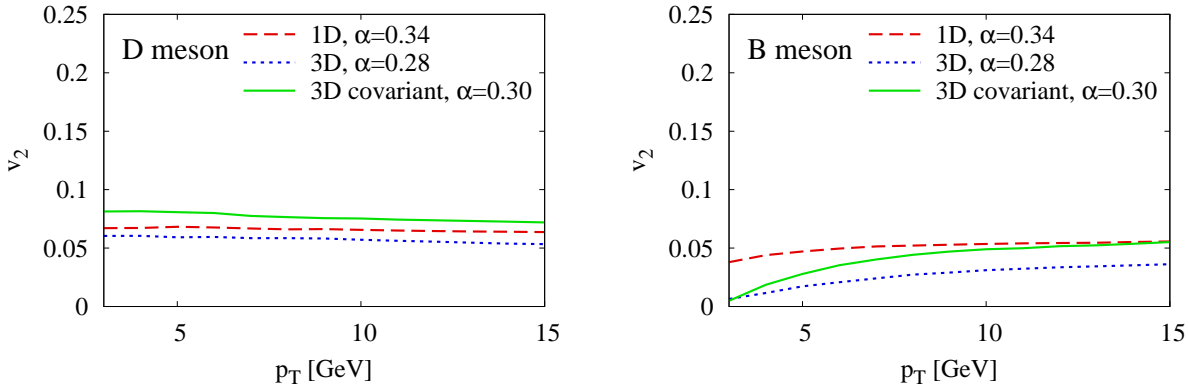


Figure 3: D (left) and B (right) meson differential elliptic flow $v_2(p_T)$ at midrapidity in mid-peripheral ($b \approx 7.5\text{ fm}$) Au+Au collisions at $\sqrt{s_{NN}} = 200$ GeV at RHIC, calculated using DGLV parton energy loss.

We also recalculated neutral pion observables in [39] for Au+Au at $\sqrt{s_{NN}} = 200$ GeV (RHIC) and Pb+Pb at $\sqrt{s_{NN}} = 2.76$ TeV (LHC) with covariant GLV energy loss using scale dependent (running) coupling

$$\alpha_s(Q^2) = \begin{cases} \alpha_{max} & , \quad \text{for } Q < Q_{min} \\ \frac{4\pi}{\beta_0 \ln(Q^2/\Lambda^2)} & , \quad \text{for } Q \geq Q_{min} \end{cases} \quad (8)$$

with $\beta_0 = 11 - 2N_f/3 = 9$ (for three light flavors), $Q_{min} = \Lambda \exp(2\pi/\alpha_{max}\beta_0)$, and $\Lambda = 0.2$ GeV. As Ref. [43], in $\sigma_{gg} = 9\pi\alpha_s^2/2\mu^2$ we used $\alpha_s^2(q^2)$, while in the prefactor, $\alpha_s(Q^2)$ with $Q^2 \approx k^2/x_+(1-x_+)$ (gluon radiation vertex). Unlike the Columbia University group, at both RHIC and LHC we found negligible running coupling effects in $R_{AA}(p_T)$ and $v_2(p_T)$ once α_{max} was tuned to reproduce R_{AA} at $p_T = 10$ GeV, except for a few percent reduction of pion v_2 at RHIC. The difference may be due to our covariant treatment, or because we did not include elastic energy loss.

1.4.3 Covariant energy loss in small p+A systems

We also performed covariant calculations for proton-lead collisions at the LHC. Following Ref. [42] we used a small ensemble of fluctuating initial conditions generated via the GLISSANDO package[45], which were then evolved with ideal hydrodynamics using our 2+1D Bjorken boost invariant solver MPC/Hydro. Geometric fluctuations arise because nuclei contain a finite number of nucleons, and also because particle production in an individual nucleon-nucleon collision is a stochastic process. For the 3.4% most central p+Pb events, we found the nuclear suppression factor noticeably below unity (e.g., R_{AA} at 10 GeV is ~ 0.9). Whereas harmonic flow coefficients v_2 and v_3 were nonzero but small at moderately high $p_T \sim 5 - 10$ GeV, less than 1% in magnitude even when geometry fluctuations were included.

Results in Section 1.4 form a major part of Deke Sun’s Ph.D. thesis. These were presented, in parts, at the Winter Workshop on Nuclear Dynamics (Jan 2015), the CIPANP conference (May 2015), and at Quark Matter 2015 (Sep 2015), and are being prepared for publication.

1.5 Presentations and publications

Publications and presentations from Year 5 of the ECRP are listed below.

Conferences/workshops:

- 1) poster - Deke Sun & Denes Molnar, “Frame independent formulation of energy loss in evolving bulk medium”, Quark Matter, May 19-24, 2014, Darmstadt, Germany
- 2) poster - Zack Wolff, “Self-consistent Cooper-Frye freeze-out of a viscous fluid to particles”, Quark Matter 2014 Int. Conf., May 19-24, 2014, Darmstadt, Germany
- 3) invited talk - Denes Molnar, “Jet energy loss and fluid dynamics”, Workshop on Jet Modification in the RHIC and LHC Era, Aug 18-20, 2014, Wayne State University, Detroit, Michigan
- 4) talk - Deke Sun, “Interplay between bulk medium evolution and covariant (D)GLV energy loss”, 31st Winter Workshop on Nuclear Dynamics (WWND2015), Jan 26-31, 2015, Keystone, Colorado
- 5) invited talk - Denes Molnar, “Viscous corrections from nonlinear transport”, 6th Workshop of the APS Topical Group on Hadronic Physics, Apr 8-10, 2015, Baltimore, MD
- 6) invited talk - Denes Molnar, “Jet quenching and fluid dynamics”, 12th Conference on the Intersections of Particle and Nuclear Physics (CIPANP 2015), May 19-24, Vail, Colorado
- 7) talk - Mridula Damodaran, ”Viscous Corrections from Nonlinear Transport”, XXVIII Midwest Theory Get-Together, Argonne National Laboratory, Sep 11-12, 2015
- 8) invited talk - Denes Molnar, “Small systems and jet energy loss”, Symposium on Looking Beyond 1010 Mini-Bangs, CGCs, Perfect Fluids, and Jet Tomo/Holo-graphy; East Lake Conference Center, Sep 25-26, 2015, Wuhan, China
- 9) poster - Dustin Hemphill, “Radiative $ggg \leftrightarrow gg$ transport and thermalization”, Quark Matter 2015 Int. Conf., Sep 27 - Oct 3, 2015, Kobe, Japan
- 10) poster - Deke Sun, “Covariant (D)GLV energy loss in proton-lead collisions at the LHC”, Quark Matter 2015 Int. Conf., Sep 27 - Oct 3, 2015, Kobe, Japan

11) invited talk - Denes Molnar, “Dissipative phase space correction δf models vs nonlinear kinetic theory”, 15th Zimányi School, Wigner RCP, Dec 7-11, 2015, Budapest, Hungary

Seminars:

- 1) Denes Molnar, “Elliptic flow from anisotropic escape”, Brookhaven National Laboratory, Jun 2, 2015, Upton, NY
- 2) Denes Molnar, “Elliptic flow from anisotropic escape”, Columbia U., Jun 3, 2015, New York, NY

Refereed publications from ECRP Year 5:

- 1) L. He, T. Edmonds, Z. W. Lin, F. Liu, D. Molnar and F. Wang, “Anisotropic parton escape is the dominant source of azimuthal anisotropy in transport models,” *Phys. Lett. B* **753**, 506 (2016) [arXiv:1502.05572 [nucl-th]].
- 2) D. Molnar, F. Wang and C. H. Greene, “Momentum anisotropy in nuclear collisions from quantum mechanics,” arXiv:1404.4119 [nucl-th], submitted to *Phys. Rev. Lett.*

Other publications from ECRP Year 5:

- 3) Z. Wolff, “Self-consistent conversion of a viscous fluid to particles and heavy-ion physics applications” (Ph.D. thesis), Purdue University, Dec 2015
- 4) D. Hemphill, “Radiative transport in heavy-ion collisions” (Ph.D. thesis), Purdue University, in preparation (exp. Aug 2016)
- 5) D. Sun, “Covariant (D)GLV energy loss in quark-gluon plasma” (Ph.D. thesis), Purdue University, in preparation (exp. Aug 2016)

2 List of references

- [1] M. Gyulassy and L. McLerran, “New forms of QCD matter discovered at RHIC,” *Nucl. Phys. A* **750**, 30 (2005) [nucl-th/0405013].
- [2] D. Molnar and M. Gyulassy, “Saturation of elliptic flow and the transport opacity of the gluon plasma at RHIC,” *Nucl. Phys. A* **697**, 495 (2002) [*Nucl. Phys. A* **703**, 893 (2002)] [nucl-th/0104073].
- [3] Z. Xu and C. Greiner, “Thermalization of gluons in ultrarelativistic heavy ion collisions by including three-body interactions in a parton cascade,” *Phys. Rev. C* **71**, 064901 (2005) [hep-ph/0406278].
- [4] J. W. Chen, H. Dong, K. Ohnishi and Q. Wang, “Shear Viscosity of a Gluon Plasma in Perturbative QCD,” *Phys. Lett. B* **685**, 277 (2010) [arXiv:0907.2486 [nucl-th]]
- [5] J. W. Chen, J. Deng, H. Dong and Q. Wang, “How Perfect a Gluon Plasma Can Be in Perturbative QCD?,” *Phys. Rev. D* **83**, 034031 (2011) [*Phys. Rev. D* **84**, 039902 (2011)] [arXiv:1011.4123 [hep-ph]].

- [6] J. F. Gunion and G. Bertsch, “Hadronization By Color Bremsstrahlung,” *Phys. Rev. D* **25**, 746 (1982).
- [7] L. D. Landau and I. Pomeranchuk, “Limits of applicability of the theory of bremsstrahlung electrons and pair production at high-energies,” *Dokl. Akad. Nauk Ser. Fiz.* **92**, 535 (1953)
- [8] A. B. Migdal, “Bremsstrahlung and pair production in condensed media at high-energies,” *Phys. Rev.* **103**, 1811 (1956)
- [9] R. Baier, Y. L. Dokshitzer, A. H. Mueller, S. Peigne and D. Schiff, “Radiative energy loss and $p(T)$ broadening of high-energy partons in nuclei,” *Nucl. Phys. B* **484**, 265 (1997) [hep-ph/9608322].
- [10] T. S. Biro, E. van Doorn, B. Muller, M. H. Thoma and X. N. Wang, “Parton equilibration in relativistic heavy ion collisions,” *Phys. Rev. C* **48**, 1275 (1993) [nucl-th/9303004].
- [11] D. Molnar and Z. Wolff, “Self-consistent conversion of a viscous fluid to particles,” arXiv:1404.7850 [nucl-th], to appear in *Phys. Rev. C*
- [12] P. Huovinen and D. Molnar, “The Applicability of causal dissipative hydrodynamics to relativistic heavy ion collisions,” *Phys. Rev. C* **79**, 014906 (2009) [arXiv:0808.0953 [nucl-th]].
- [13] P. Romatschke and M. Strickland, “Collisional energy loss of a heavy quark in an anisotropic quark-gluon plasma,” *Phys. Rev. D* **71**, 125008 (2005) [hep-ph/0408275].
- [14] W. Florkowski, E. Maksymiuk, R. Ryblewski and M. Strickland, “Exact solution of the (0+1)-dimensional Boltzmann equation for a massive gas,” *Phys. Rev. C* **89**, no. 5, 054908 (2014) [arXiv:1402.7348 [hep-ph]].
- [15] P. Huovinen and P. V. Ruuskanen, “Hydrodynamic Models for Heavy Ion Collisions,” *Ann. Rev. Nucl. Part. Sci.* **56**, 163 (2006) [nucl-th/0605008]
- [16] D. A. Teaney, “Viscous Hydrodynamics and the Quark Gluon Plasma,” arXiv:0905.2433 [nucl-th]
- [17] C. Gale, S. Jeon and B. Schenke, “Hydrodynamic Modeling of Heavy-Ion Collisions,” *Int. J. Mod. Phys. A* **28**, 1340011 (2013) [arXiv:1301.5893 [nucl-th]].
- [18] D. Molnar, “Identified particles from viscous hydrodynamics,” *J. Phys. G* **38**, 124173 (2011) [arXiv:1107.5860 [nucl-th]].
- [19] Z. Wolff and D. Molnar, “Self-consistent Cooper-Frye freeze-out of a viscous fluid to particles,” *J. Phys. Conf. Ser.* **535**, 012020 (2014) doi:10.1088/1742-6596/535/1/012020 [arXiv:1407.6413 [nucl-th]].
- [20] Z. Wolff, “Self-consistent conversion of a viscous fluid to particles and heavy-ion physics applications” (Ph.D. thesis), Purdue University, Dec 2015
- [21] The original version 0.2 of AZHYDRO and version 0.2p2 patched by P. Huovinen and D. Molnar are available on the WWW from the Open Standard Codes and Routines (OSCAR) repository at <http://karman.physics.purdue.edu/OSCAR>
- [22] P. F. Kolb, J. Sollfrank and U. W. Heinz, “Anisotropic transverse flow and the quark hadron phase transition,” *Phys. Rev. C* **62**, 054909 (2000) [hep-ph/0006129]

- [23] P. F. Kolb and R. Rapp, “Transverse flow and hadrochemistry in Au+Au collisions at $(S(NN))^{**}(1/2) = 200\text{-GeV}$,” *Phys. Rev. C* **67**, 044903 (2003) [hep-ph/0210222];
- [24] P. F. Kolb and U. W. Heinz, “Hydrodynamic description of ultrarelativistic heavy ion collisions,” In *Hwa, R.C. (ed.) et al.: Quark gluon plasma* 634-714 [nucl-th/0305084].
- [25] R. Paatelainen, K.J. Eskola, H. Niemi, K. Tuominen, “Fluid dynamics with saturated minijet initial conditions in ultrarelativistic heavy-ion collisions”, *Phys. Lett. B* **731**, 126 (2014)
- [26] H. Niemi, G.S. Denicol, H. Holopainen, P. Huovinen, “Event-by-event distributions of azimuthal asymmetries in ultrarelativistic heavy-ion collisions”, *Phys. Rev. C* **87**, 054901 (2013)
- [27] H. Niemi *et al*, “Influence of a temperature-dependent shear viscosity on the azimuthal asymmetries of transverse momentum spectra in ultrarelativistic heavy-ion collisions”, *Phys. Rev. C* **86**, 014909 (2012)
- [28] H. Niemi *et al*, “Influence of shear viscosity of quark-gluon plasma on elliptic flow in ultrarelativistic heavy-ion collisions”, *Phys. Rev. Lett* **106**, 212302 (2011)
- [29] D. Molnar, F. Wang and C. H. Greene, “Momentum anisotropy in nuclear collisions from quantum mechanics,” arXiv:1404.4119 [nucl-th], submitted to *Phys. Rev. Lett.*
- [30] B. Zhang, C.M. Ko, B.-A. Li, and Z.-W. Lin, *Phys. Rev. C* **61**, 067901 (2000).
- [31] Z.-W. Lin, C.M. Ko, B.-A. Li, B. Zhang, and S. Pal, *Phys. Rev. C* **72**, 064901 (2005).
- [32] D. Molnar and M. Gyulassy, “New solutions to covariant nonequilibrium dynamics”, *Phys. Rev. C* **62**, 054907 (2000); D. Molnar, MPC 1.8.11. This transport code and later versions are available at <http://karman.physics.purdue.edu/OSCAR>
- [33] L. He, T. Edmonds, Z. W. Lin, F. Liu, D. Molnar and F. Wang, “Anisotropic parton escape is the dominant source of azimuthal anisotropy in transport models,” *Phys. Lett. B* **753**, 506 (2016) [arXiv:1502.05572 [nucl-th]].
- [34] D. Molnar and D. Sun, “Realistic medium-averaging in radiative energy loss,” *Nucl. Phys. A* **910-911**, 486 (2013) [arXiv:1209.2430 [nucl-th]].
- [35] D. Molnar and D. Sun, “High-pT suppression and elliptic flow from radiative energy loss with realistic bulk medium expansion,” arXiv:1305.1046 [nucl-th],
- [36] M. Gyulassy, P. Levai and I. Vitev, “Jet quenching in thin quark-gluon plasmas. I: Formalism,” *Nucl. Phys. B* **571** (2000) 197 [arXiv:hep-ph/9907461].
- [37] M. Gyulassy, P. Levai and I. Vitev, “Reaction operator approach to nonAbelian energy loss,” *Nucl. Phys. B* **594**, 371 (2001) [nucl-th/0006010]
- [38] A. Buzzatti and M. Gyulassy, “Jet Flavor Tomography of Quark Gluon Plasmas at RHIC and LHC,” *Phys. Rev. Lett.* 108 (2012) 022301, arXiv:1106.3061 [hep-ph].
- [39] D. Molnar and D. Sun, “Interplay between bulk medium evolution and (D)GLV energy loss,” *Nucl. Phys. A* **932**, 140 (2014) [arXiv:1405.4848 [nucl-th]].
- [40] M. Djordjevic and U. Heinz, “Radiative heavy quark energy loss in a dynamical QCD medium,” *Phys. Rev. C* **77** (2008) 024905 [arXiv:0705.3439 [nucl-th]].

- [41] M. Djordjevic and U. Heinz, “Radiative heavy quark energy loss in a dynamical QCD medium,” *Phys. Rev. C* **77**, 024905 (2008) [arXiv:0705.3439 [nucl-th]].
- [42] P. Bozek and W. Broniowski, “Collective dynamics in high-energy proton-nucleus collisions,” *Phys. Rev. C* **88**, no. 1, 014903 (2013) [arXiv:1304.3044 [nucl-th]].
- [43] J. Xu, A. Buzzatti and M. Gyulassy, “Azimuthal jet flavor tomography with CUJET2.0 of nuclear collisions at RHIC and LHC,” *JHEP* **1408**, 063 (2014) [arXiv:1402.2956 [hep-ph]].
- [44] C. Peterson, D. Schlatter, I. Schmitt and P. M. Zerwas, “Scaling Violations in Inclusive e+ e- Annihilation Spectra,” *Phys. Rev. D* **27**, 105 (1983).
- [45] M. Rybczynski, G. Stefanek, W. Broniowski and P. Bozek, “GLISSANDO 2 : GLauber Initial-State Simulation AND mOre, ver. 2,” *Comput. Phys. Commun.* **185**, 1759 (2014) [arXiv:1310.5475 [nucl-th]].